Supporting Information

Tris(allyl)indium Compounds: Synthesis and Structural Characterization

Ilja Peckermann, Gerhard Raabe, Thomas P. Spaniol and Jun Okuda*

Synthesis and characterization

All operations were performed under an inert atmosphere of argon using standard Schlenk-line or glovebox techniques. 1,4-dioxane, THF and pentane were distilled under argon from sodium/benzophenone ketyl prior to use. Anhydrous indium trichloride (ABCR) as well as allyl- and 2-methylallyl Grignard solutions in THF (Aldrich) were used as received. Benzene-d_6 and THF-d_8 were dried and stored in a glovebox. NMR spectra were recorded on a Bruker Avance 400 spectrometer at the temperatures stated below.

$[In(C_3H_5)_3]$ (1a)
To a cold (0°C) solution of anhydrous $InCl_3$ (2.0 g, 9.02 mmol) in THF (70 mL), a cooled (0°C) 2.0 M THF solution of C_3H_5MgCl (13.58 mL, 27.06 mmol) was added. The mixture was stirred for 5 h at 0°C, followed by addition of 40 mL of 1,4-dioxane. After the suspension was stirred overnight at 0°C, the precipitate was separated by filtration and the solvent was removed *in vacuo*. Drying the product under reduced pressure gave a yellow oil in 44% yield (1.30 g, 3.99 mmol).
Anal. C 45.50 %, H 6.61 %
Calcd. $C_9H_{15}In$: C 45.41%, H 6.35 %

$[In(C_4H_7)_3]$ (1b)
To a solution of anhydrous $InCl_3$ (500 mg, 2.26 mmol) in a mixture of THF (10 mL) and 1,4-dioxane (10 mL), a 0.5 M THF solution of C_4H_7MgCl (13.5 mL, 6.78 mmol) at 0°C was slowly added and the mixture was stirred for 16 h at 0°C. After filtration of the precipitate and removing the solvent *in vacuo*, the product was washed with *n*-pentane and dried under reduced pressure to give a colorless solid in a yield of 64% (410 mg, 1.45 mmol). Single crystals were grown from *n*-pentane at –30°C.
Anal.: C 49.90 %, H 7.41 %
Calcd.: $C_{12}H_{21}In$: C 51.45 %, H 7.56 %
We explain the deviation between the experimental value and the calculated value by the high sensitivity of this compound.

$[In(C_3H_5)_2Cl(diox)]$ (2a)
To a solution of anhydrous indium trichloride (2.0 g, 9.04 mmol) in 70 mL of THF, a 2.0 M THF solution of C_3H_5MgCl (9.04 mL, 18.04 mmol) was slowly added at 0°C and the mixture was stirred at this temperature for 17 h. After addition of 40 mL of 1,4-dioxane, the precipitate was filtered, the solvent was removed and the product was dried *in vacuo* at 0°C to give a colorless solid in 48% yield (1.40 g, 4.37 mmol).
Anal.: C 37.60 %, H 5.64 %
Calcd.: $C_{10}H_{18}ClInO_2$: C 37.47 %, H 5.66 %

$[In(C_3H_5)Cl_2(diox)]$ (3a)
To a solution of anhydrous indium trichloride (1.0 g, 4.5 mmol) in a mixture of 7.0 mL of THF and 2.0 mL of 1,4-dioxane, a 2.0 M THF solution of C_3H_5MgCl (2.3 mL, 4.5 mmol) was slowly added and stirred for 16 hours. After filtration of the precipitate, the solvent was removed *in vacuo* and the product was dried under reduced pressure to give a colorless solid in a yield of 71% (1.01 g, 3.2 mmol).
Anal.: C 27.13 %, H 4.08 %
Calcd.: $C_7H_{13}Cl_2InO_2$: C 26.70 %, H 4.16 %

$[In(C_4H_7)_2Cl]$ (2b)
To a solution of anhydrous indium trichloride (500 mg, 2.26 mmol) in a 1:1 mixture of 4.0 mL of THF and 1,4-dioxane, a 0.5 M THF solution of C_4H_7MgCl (9.0 mL, 4.52 mmol) was slowly added at 0°C. The solution was stirred for 16 h at ambient temperature. After filtration of the precipitate, the solvent was removed *in vacuo* and the product washed with *n*-pentane. Drying under reduced pressure gave a colorless solid in a yield of 73% (260 mg, 1.0 mmol).
Anal.: C 35.83 %, H 5.29 %
Calcd.: $C_8H_{14}ClIn$: C 36.89 %, H 5.42 %

$[In(C_4H_7)Cl_2]$ (3b)
To a solution of anhydrous indium trichloride (500 mg, 2.26 mmol) in a 1:1 mixture of 4.0 mL of THF and 1,4-dioxane, a 0.5 M THF solution of C_4H_7MgCl (4.5 mL, 2.26 mmol) was slowly added and stirred overnight (16 h) at ambient temperature. After filtration of the precipitate, the solvent was removed *in vacuo* and the product was washed with *n*-pentane. Drying under reduced pressure gave a colorless solid in a yield of 83% (450 mg, 1.87 mmol).
Anal.: C 20.46 %, H 3.42 %
Calcd.: $C_4H_7Cl_2In$: C 19.95 %, H 2.93 %

NMR spectra of $[In(C_3H_5)_3]$ (1a)

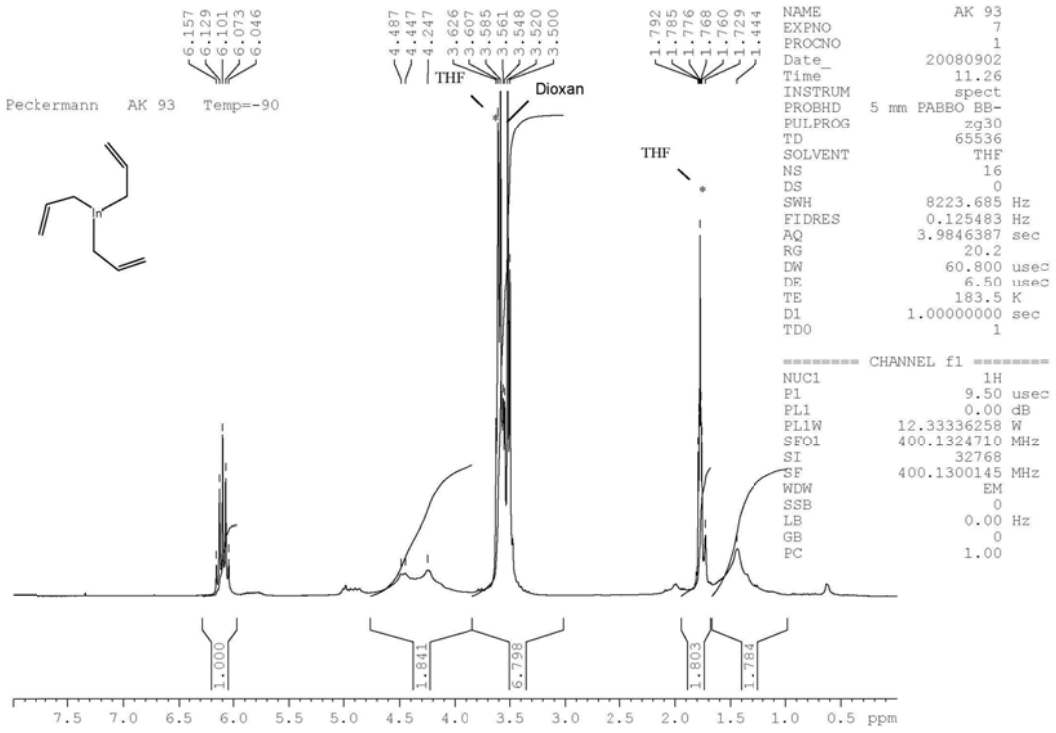

Figure S1: ^{1}H-NMR spectrum of **1a** (THF-d^8, –90°C)
δ = 1.44 (br s, 6H, $InCH_2$), 3.59 (m, $C_4H_8O_2$), 4.25 (br, 3 H, CH=C*H*H), 4.46 (br, 3 H, CH=C*H*H), 6.10 (m, 3 H, *J* = 11 Hz, C*H*=CH_2) ppm.
At −90°C, the ^{1}H NMR spectrum indicates η^1-coordination of the allyl ligands.

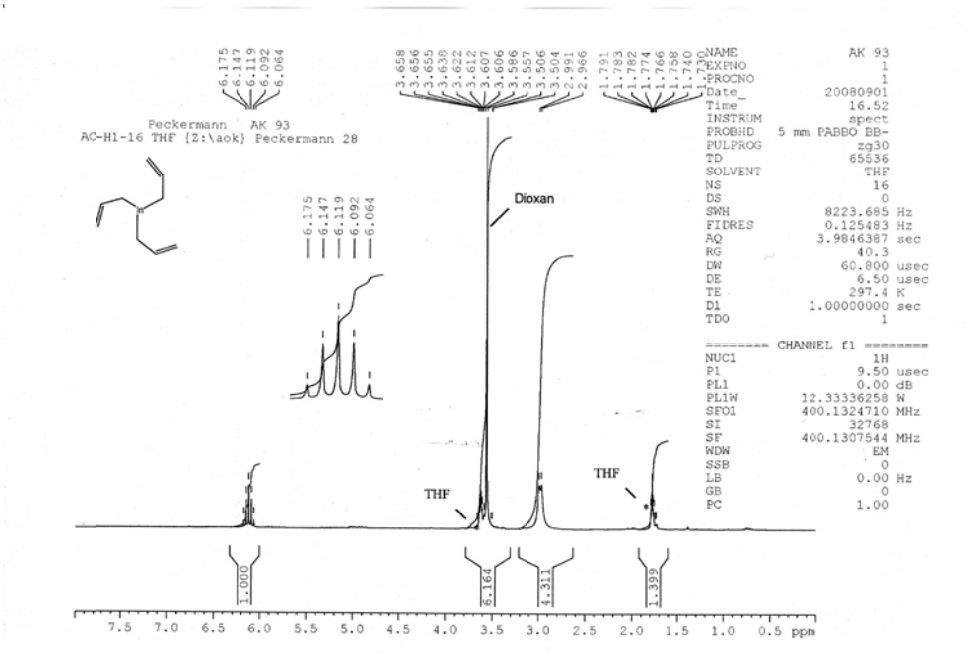

Figure S2: ^{1}H-NMR spectrum of **1a** (THF-d^8, +24°C)
δ = 2.98 (d, 12 H, *J* = 11 Hz, CH_2), 3.56 (s, $C_4H_8O_2$), 6.12 (m, 3 H, *J* = 11 Hz, CH) ppm.
At room temperature, fast exchange leads to an averaged signal for the CH_2 protons at δ = 3 ppm.

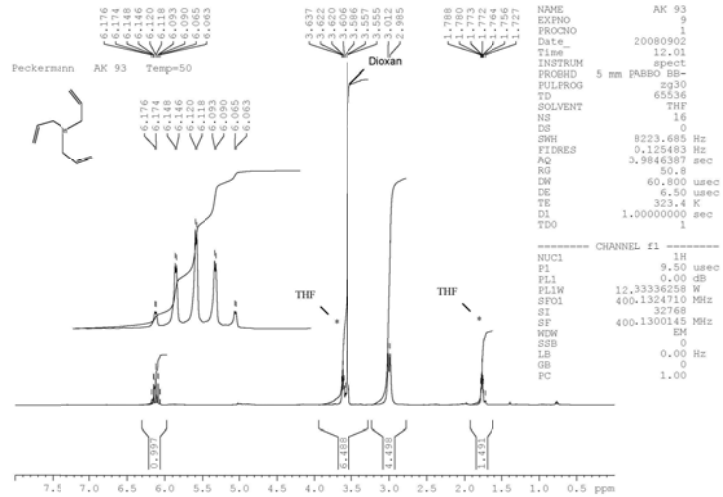

Figure S3: ^{1}H-NMR spectrum of **1a** (THF-d^{8}, +50°C):
δ = 3.0 (d, 12 H, *J* = 11 Hz, CH_2), 3.56 (s, $C_4H_8O_2$), 6.12 (m, 3 H, *J* = 11 Hz, CH) ppm.
The doublet structure of the signal at δ = 3 ppm is pronounced at this temperature

---

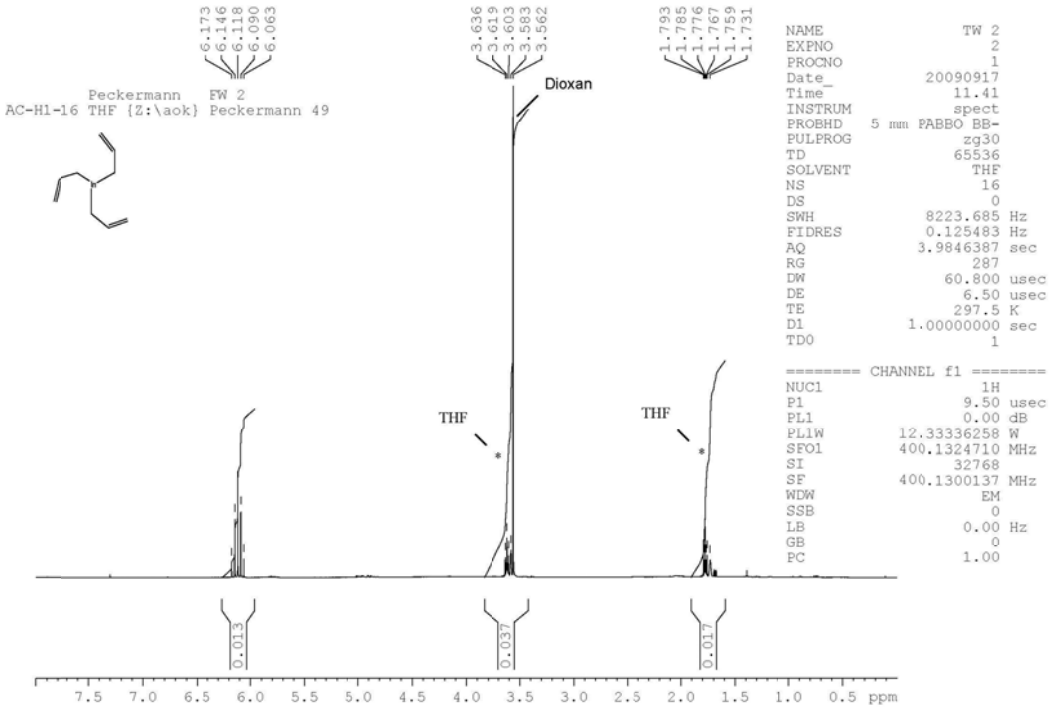

Figure S4: ^{1}H-NMR spectrum of **1a** (THF-d^{8}, +25°C):
δ = 3.56 (s, $C_4H_8O_2$), 6.12 (m, 3 H, *J* = 11 Hz, CH) ppm.
No signal for CH_2 can be extracted from this spectrum because this signal is too broad.
This ^{1}H NMR spectrum, recorded at room temperature shows that the signal for the CH_2 protons at δ = 3 ppm may not always be observed due to signal broadening and the presence of $[In(C_3H_5)_3]$ can easily be "overlooked".

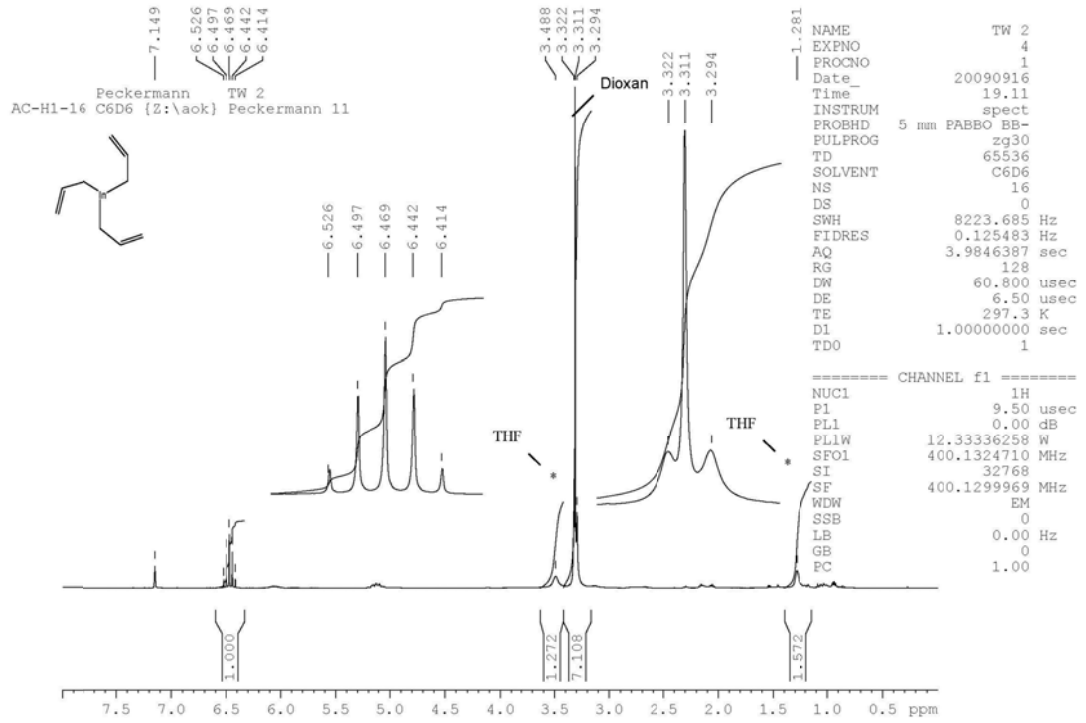

Figure S5: ^{1}H-NMR spectrum of **1a** (C_6D_6, +24°C):
δ = 3.30 (d, 12 H, *J* = 11 Hz, CH_2), 3.31 (s, $C_4H_8O_2$), 6.47 (m, 3 H, *J* = 11 Hz, CH) ppm.
The ^{1}H-NMR spectrum in C_6D_6 at room temperature clearly shows a doublet for the CH_2 protons at δ = 3.30 ppm due to fast exchange in this solvent.

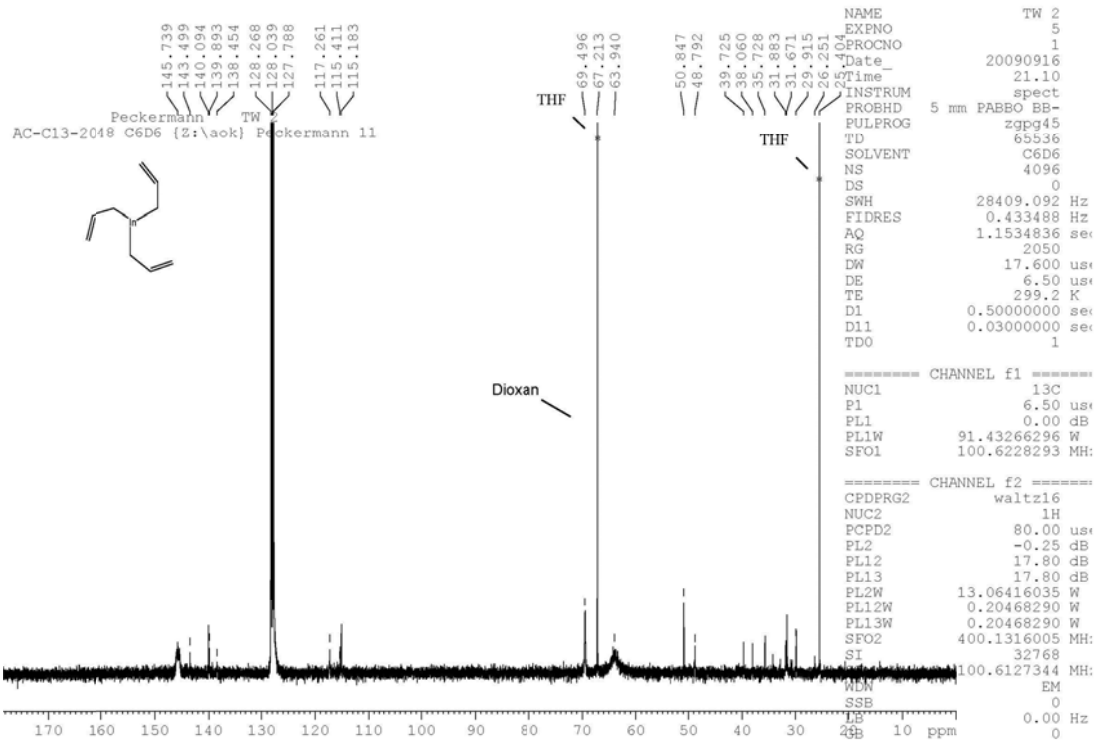

Figure S6: ^{13}C-NMR spectrum of **1a** (C_6D_6, +27°C):
δ = 63.9 (br, CH_2), 145.7 (br, C**H**) ppm.
Due to fast exchange (as observed in the ^{1}H-NMR spectrum in C_6D_6 at room temperature), only one broad resonance is observed for the carbon atoms of the CH_2 groups at δ = 63.9 ppm. Because of the very broad signals from [$In(C_3H_5)_3$], the presence of only small amounts of impurities appear enhanced.

NMR spectra of $[In(C_4H_7)_3]$ (1b)

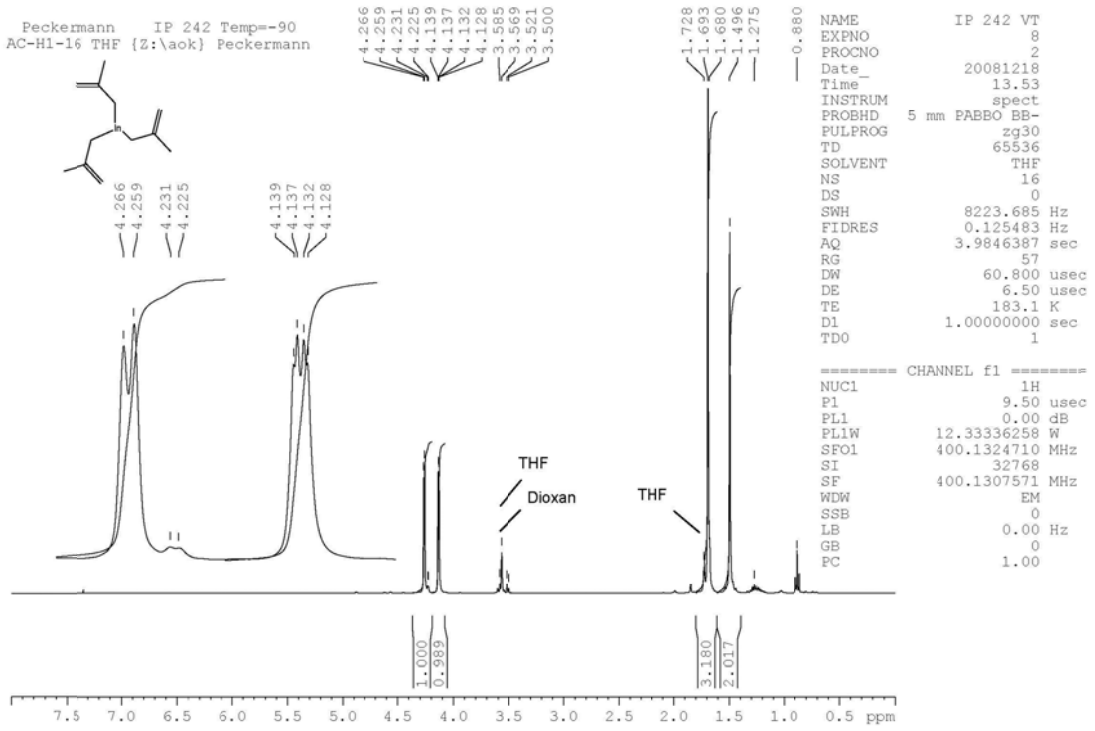

Figure S7: ^{1}H-NMR spectrum of **1b** (THF-d^8, –90°C):
δ = 1.50 (s, 6 H, $InCH_2$), 1.69 (s, 9 H, CH_3), 4.13 (m, 3 H, C=C*H*H), 4.26 (d, 3 H, J_{gem} = 3 Hz, C*H*H) ppm.
At –90°C, the ^{1}H NMR spectrum shows η^1 coordination of the allyl ligands.

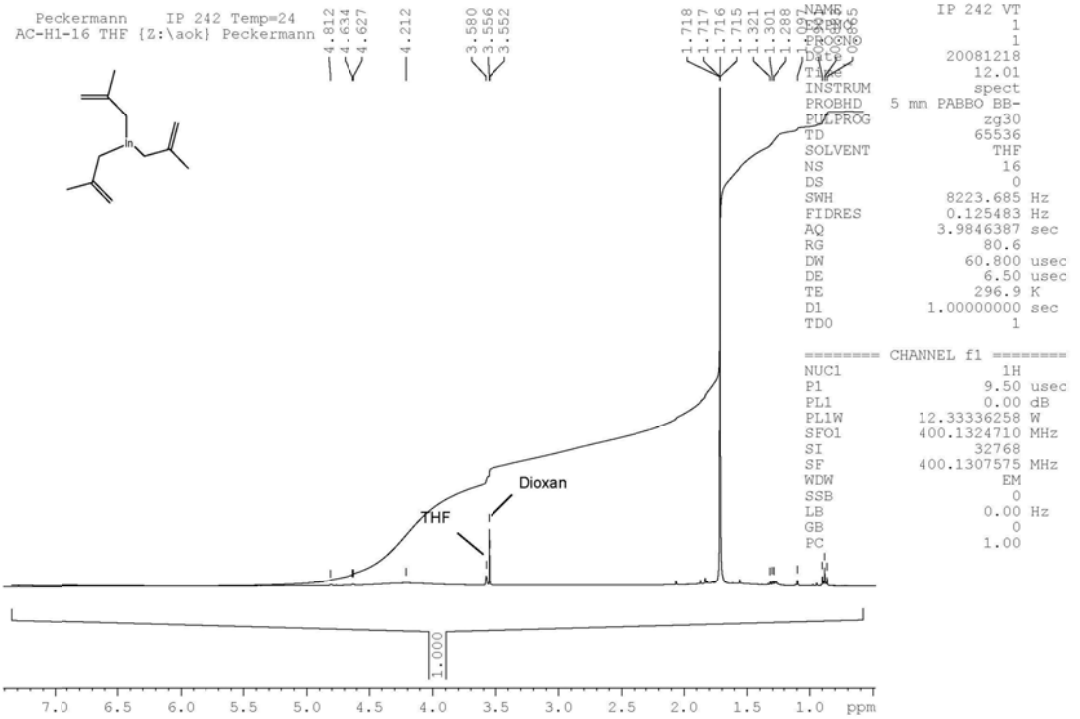

Figure S8: ^{1}H-NMR spectrum of **1b** (THF-d^8, +24°C):
δ = 1.72 (s, 9H, CH_3), 1.0 – 2.5 (br, 6 H, $InCH_2$), 3.0 – 5.0 (br, 6 H, C=CH_2) ppm.
The signals from the CH_2 groups are very broad and can hardly be observed in the ^{1}H NMR spectrum at room temperature.

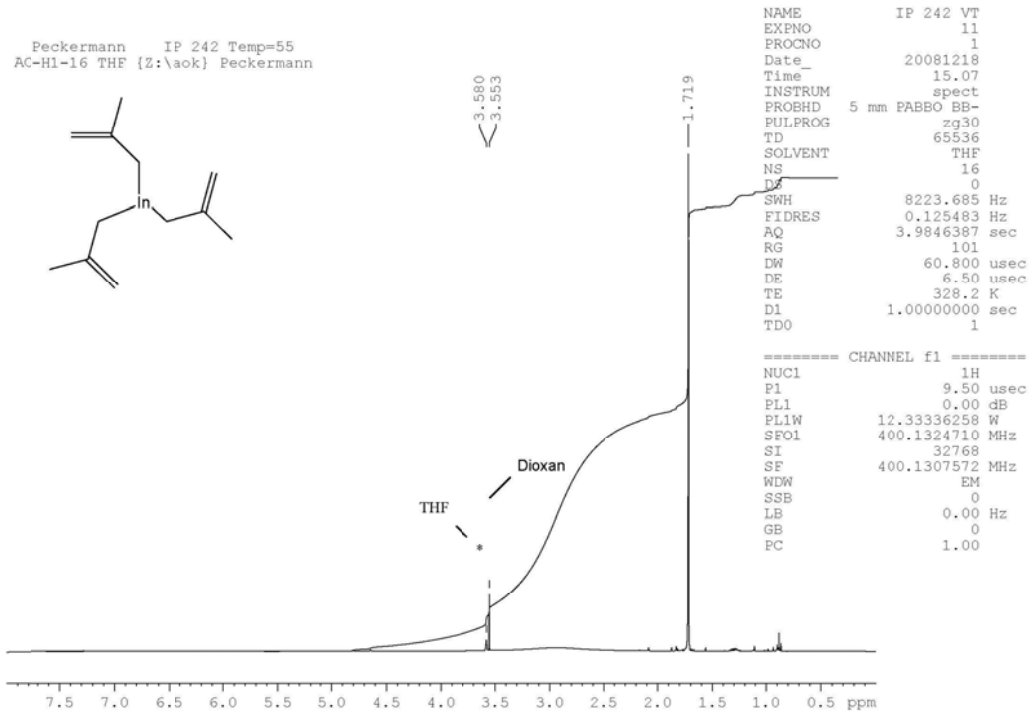

Figure S9: ^{1}H-NMR spectrum of **1b** (THF-d^{8}, +55°C):
δ = 1.72 (s, 9H, CH_3), 2.0 - 4.5 (br, 12 H, CH_2) ppm.
At elevated temperature (55°C), only one averaged signal for the CH_2 groups is observed. This signal is very broad.

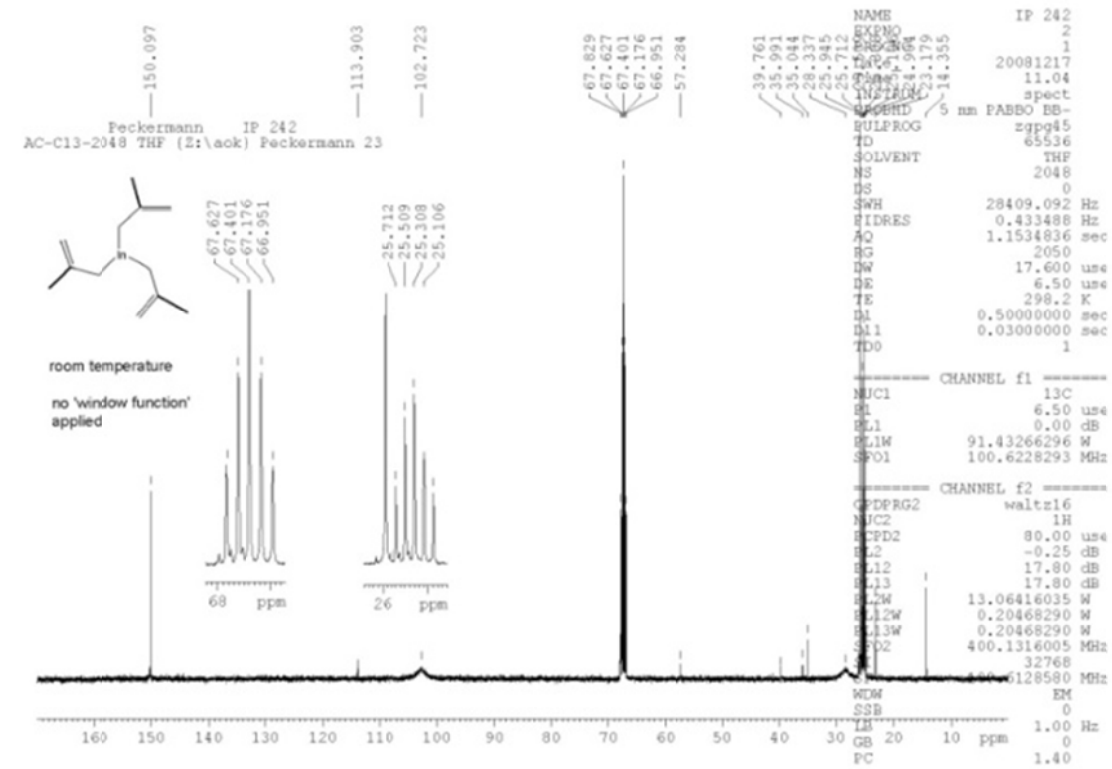

Figure S10: ^{13}C-NMR spectrum of **1b** (THF-d^{8}, +25°C):
δ = 25.9 (s, $InCH_2$), 28.3 (br s, CH_3), 102.7 (br s, C=CH_2), 150.1 (s, *C*-CH_3) ppm.
The ^{13}C NMR spectrum at room temperature in THF-d^{8} shows a broad signal for the $InCH_2$ group and also for the $=CH_2$ group.
This indicates that no fast exchange occurs at room temperature in this solvent.
Because of the very broad signals from [$In(C_4H_7)_3$], the presence of only small amounts of impurities appear enhanced.

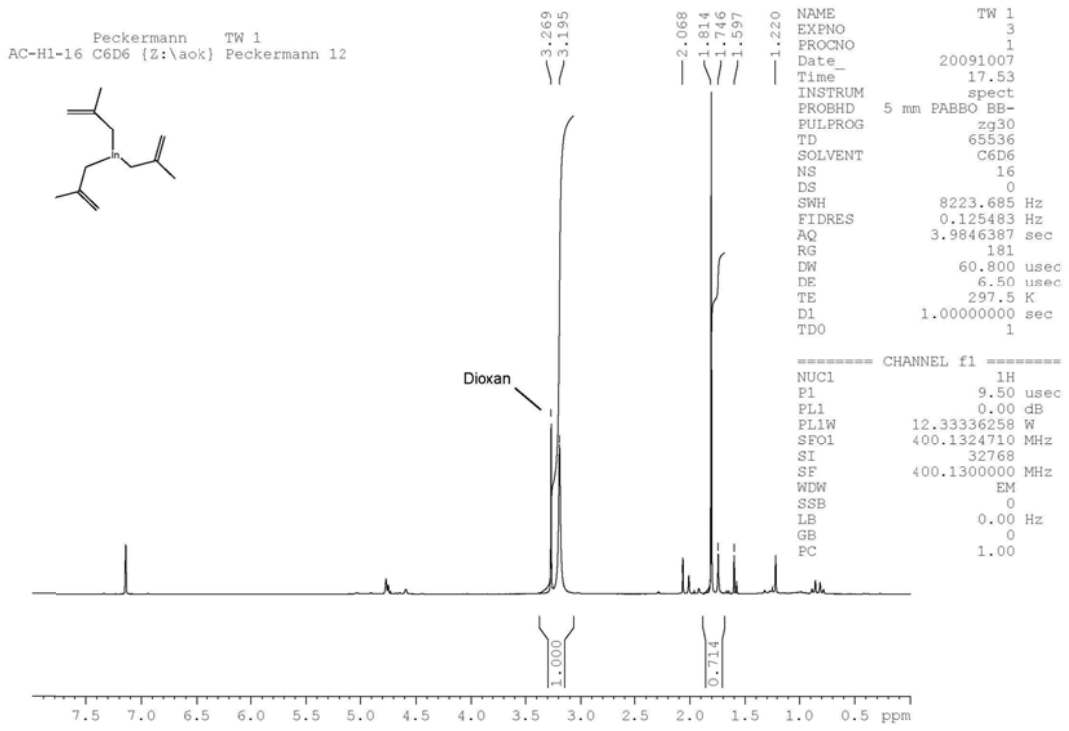

Figure S11: ^{1}H-NMR spectrum of **1b** (C_6D_6, +25°C):
δ = 1.81 (s, 12 H, CH_3), 3.19 (br s, 12 H, CH_2), 3.27 (s, $C_4H_8O_2$) ppm.
The ^{1}H-NMR spectrum at room **t**emperature in C_6D_6 shows an averaged signal at δ = 3.19 ppm from the CH_2 groups (indicating fast exchange at room temperature).

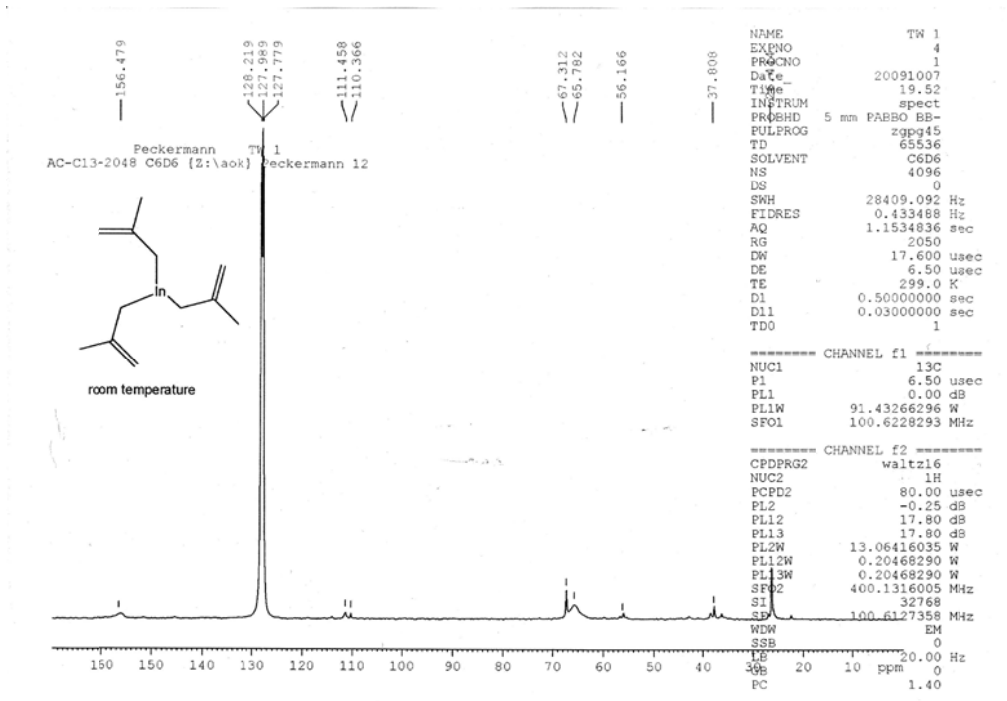

Figure S12: ^{13}C-NMR spectrum of **1b** (C_6D_6, +26°C):
δ = 26.4 (s, CH_3), 65.8 (br s, CH_2), 156.5 (br s, C=*C*H) ppm.
Due to fast exchange (as observed in the ^{1}H-NMR spectrum in C_6D_6 at room temperature), only one broad resonance is observed for the carbon atoms of the CH_2 groups at δ = 65.8 ppm. Because of the very broad signals from [$In(C_4H_7)_3$], the presence of only small amounts of impurities appears enhanced.

NMR spectra of $[InCl(C_3H_5)_2]$ (2a)

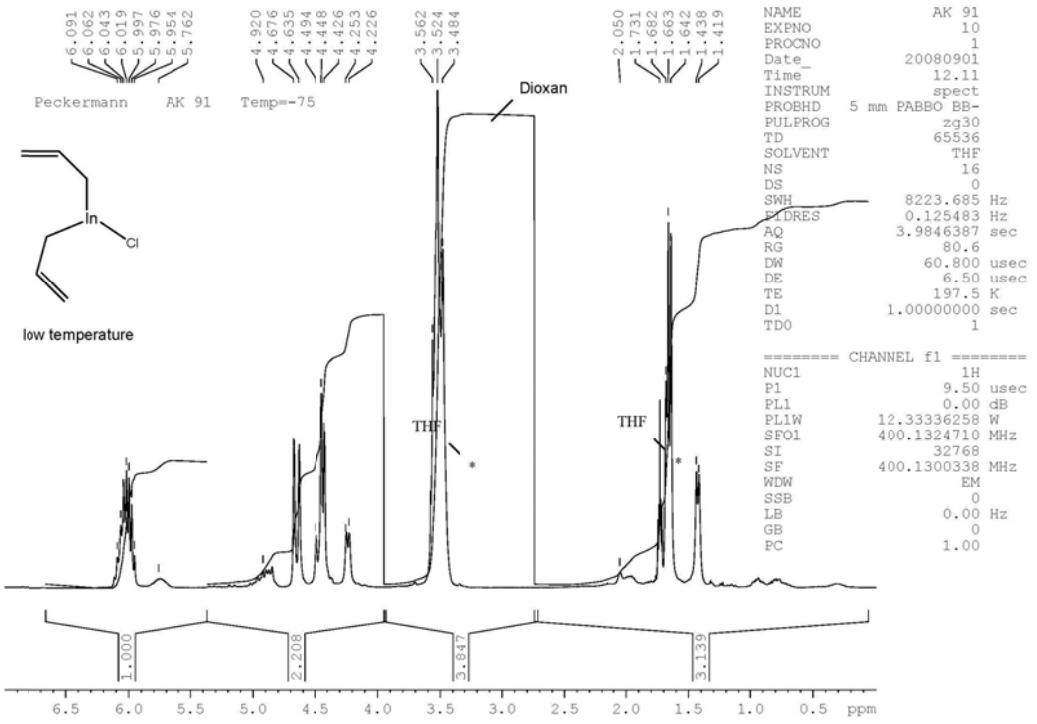

Figure S13: ^{1}H-NMR spectrum of **2a** (THF-d^8, –75°C)
δ = 1.65 (d, 4H, J = 9 Hz, $InCH_2$), 3.52 (m, $C_4H_8O_2$), 4.44 (d, 2 H, Jcis = 9 Hz, CH=CHH), 4.66 (d, 2 H, Jtrans = 16 Hz, CH=C*H*H), 6.09 (m, 2 H, C*H*=CH_2) ppm.
At −90°C, the ^{1}H NMR spectrum indicates η^1-coordination of the allyl ligands.

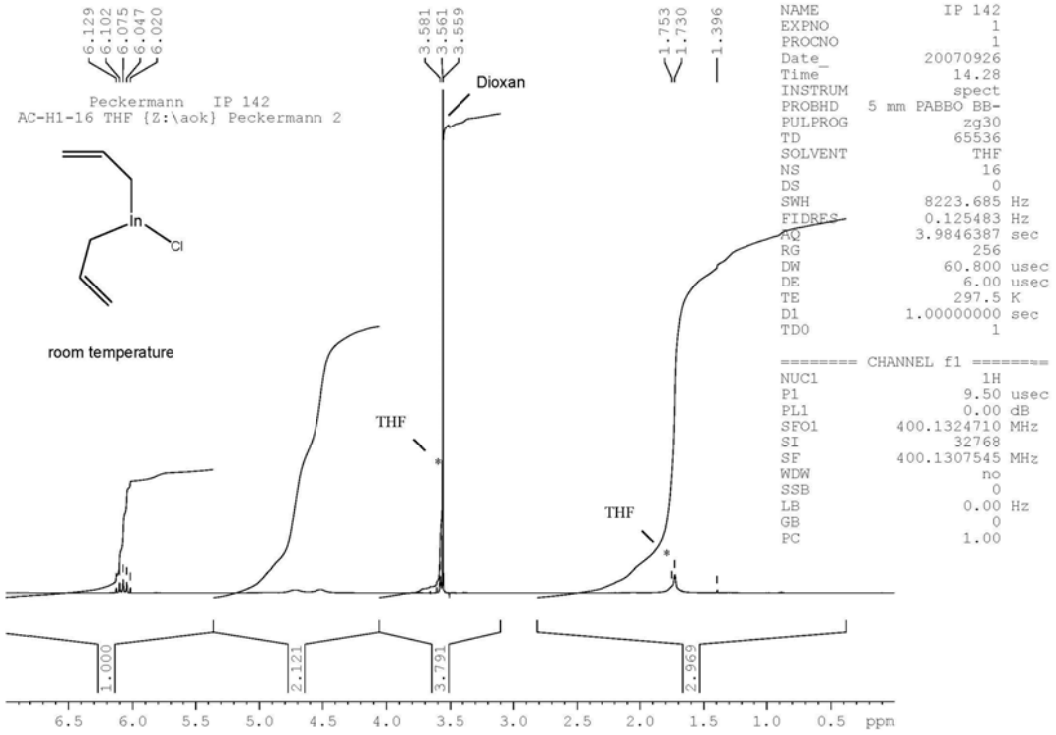

Figure S14: ^{1}H-NMR spectrum of **2a** (THF-d^8, +25°C)
δ = 1.7 (br s, 4H, J = $InCH_2$), 3.56 (m, $C_4H_8O_2$), 4.51 (br, 2 H, CH=CHH), 4.72 (br, 2 H, CH=C*H*H), 6.08 (m, 2 H, J = 11 Hz, C*H*=CH_2) ppm.

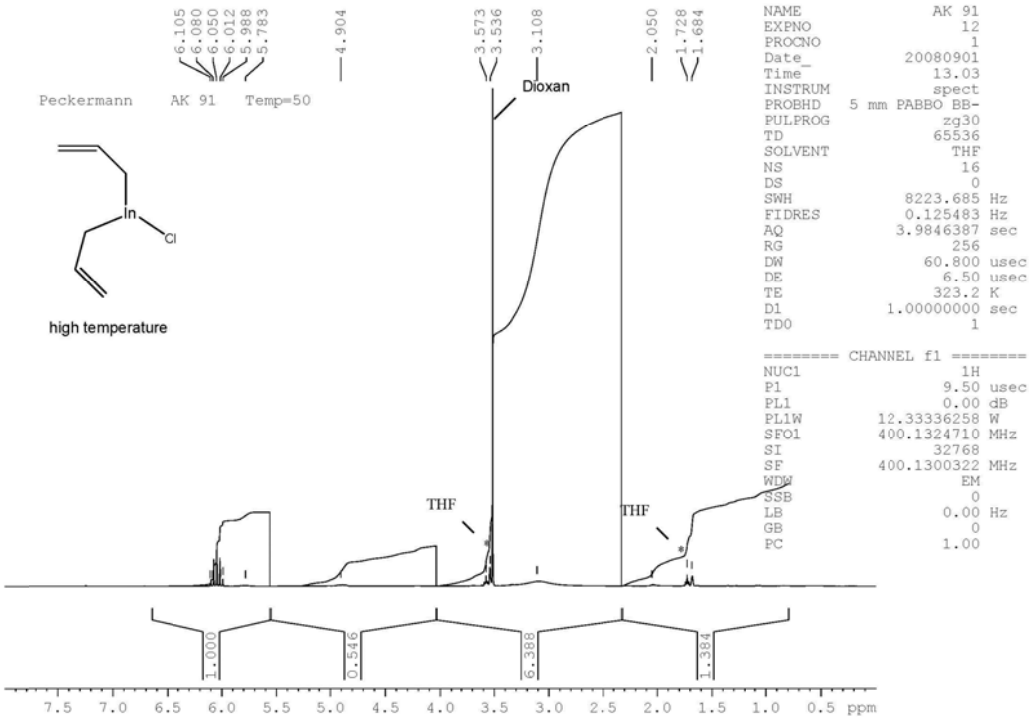

Figure S15: ^{1}H-NMR spectrum of **2a** (THF-d^{8}, +50°C)
δ = 3.11 (br, 8 H, J = CH_2), 3.54 (m, $C_4H_8O_2$), 6.05 (pent, 2 H, J = 12.0 Hz, CH) ppm.

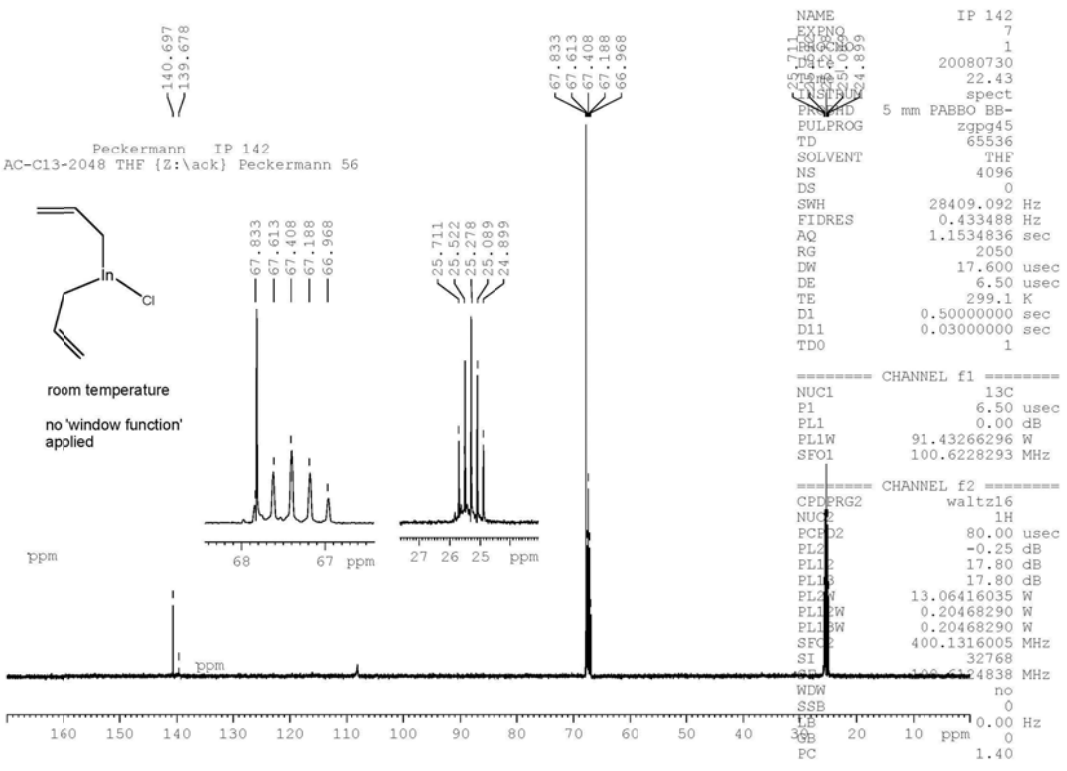

Figure S16: ^{13}C{^{1}H}-NMR spectrum of **2a** (THF-d^{8}, +26°C)
δ = 25.5 (br, $InCH_2$), 67.83 (m, $C_4H_8O_2$), 108.1 (br, $CHCH_2$), 140.7 (s, CH) ppm.

NMR spectra of [InCl(C_4H_7)$_2$] (2b)

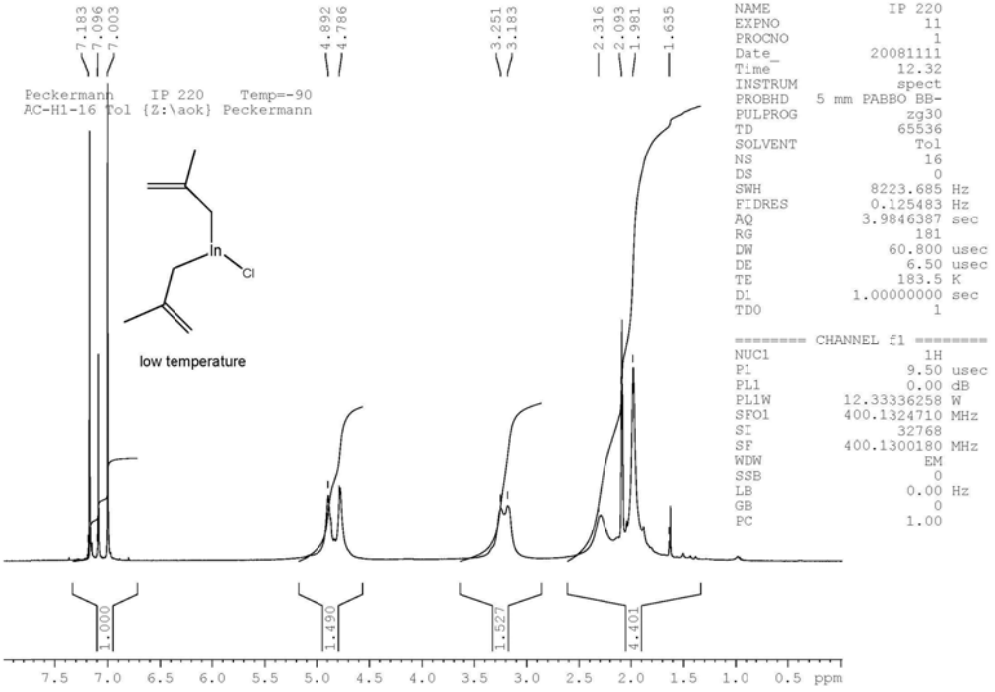

Figure S17: ^{1}H-NMR spectrum of **2b** (toluene-d^8, –90°C)
δ = 1.98 (br, 6 H, CH_3), 2.32 (br, 4 H, InCH_2), 3.18 m ($C_4H_8O_2$), 4.79 (s, 1 H, C=C*H*H), 4.89 (s, 2 H, C=CH*H*) ppm.

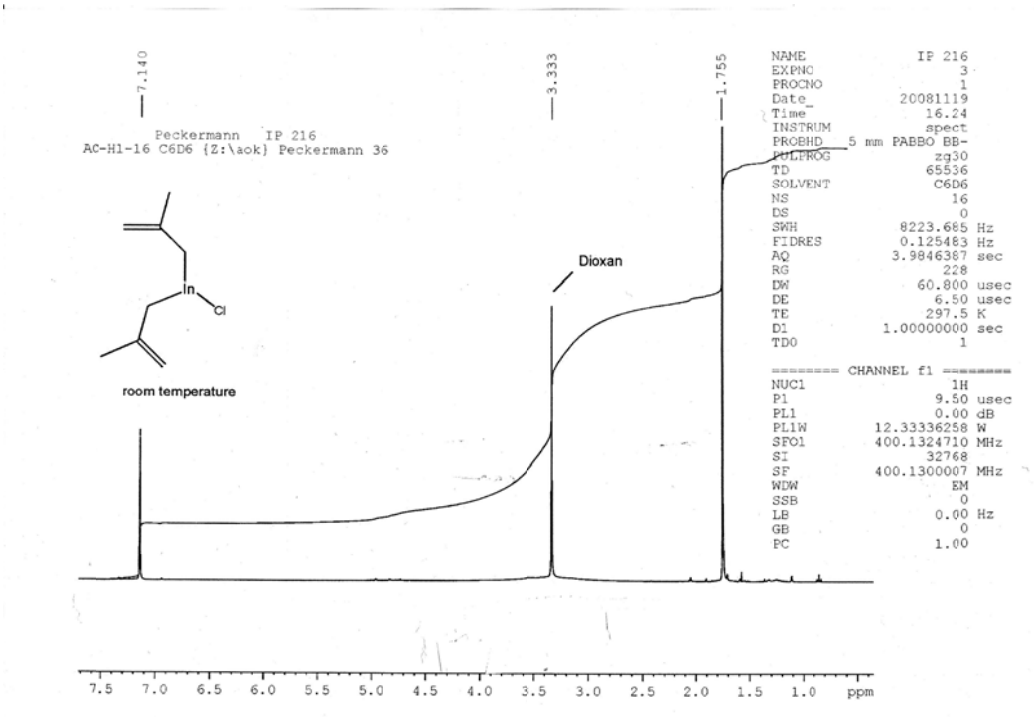

Figure S18: ^{1}H-NMR spectrum of **2b** (C_6D_6, +25°C)
δ = 1.76 (s, 6 H, CH_3), 2.0–5.5 (br, 4 H, CH_2), 3.35 s ($C_4H_8O_2$) ppm.

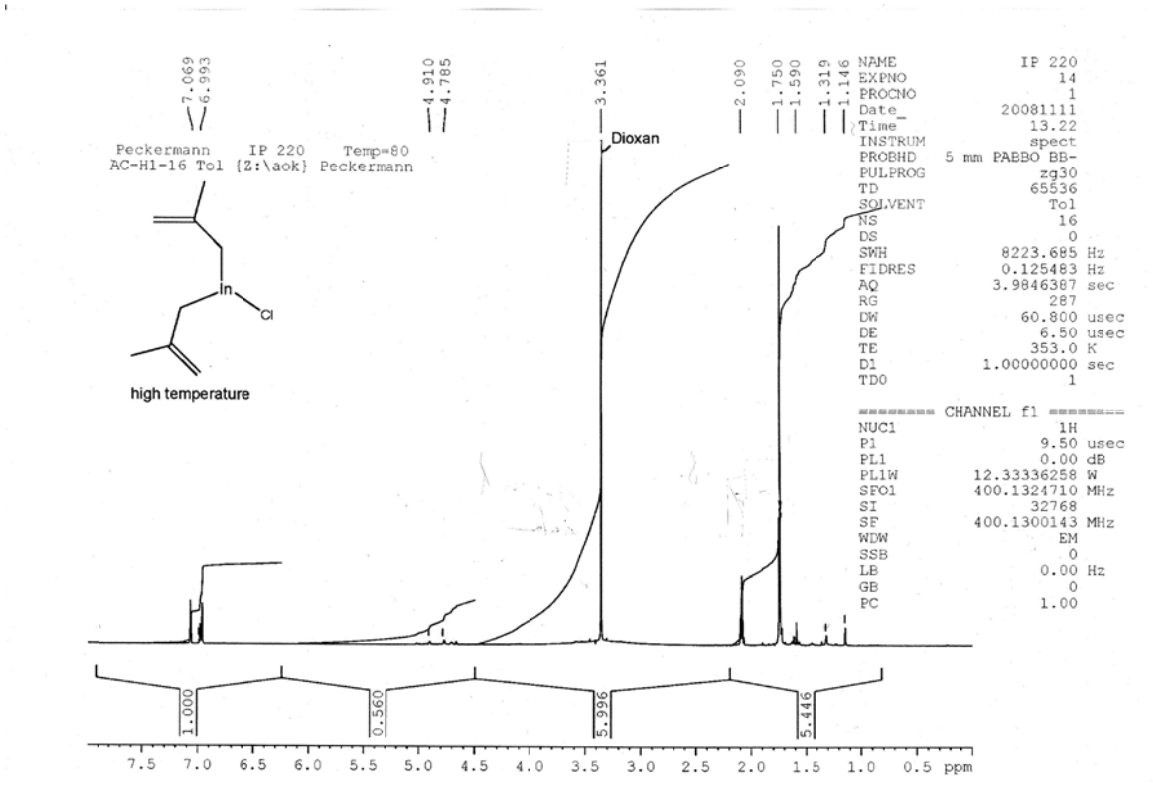

Figure S19: ^{1}H-NMR spectrum of **2b** (toluene-d^{8}, +80°C)
δ = 1.75 (s, 6 H, CH_3), 2.0–4.5 (br, 4 H, CH_2), 3.36 s ($C_4H_8O_2$) ppm.

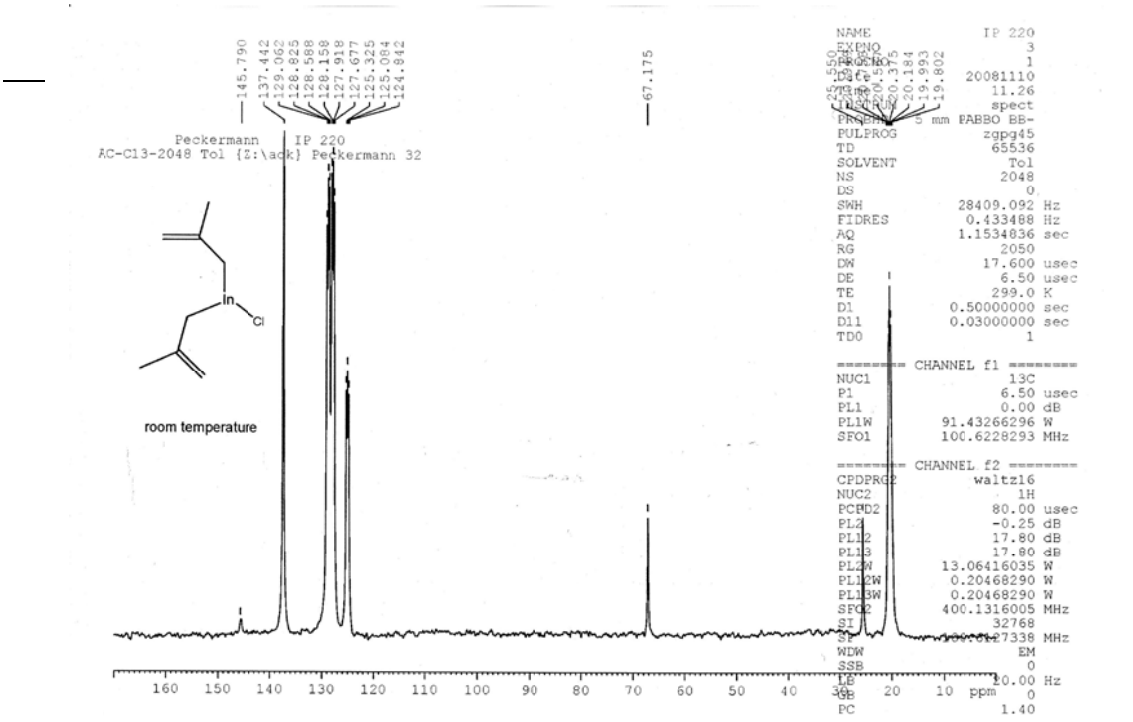

Figure S20: ^{13}C{^{1}H}-NMR spectrum of **2b** (toluene-d^{8}, +25°C)
δ = 25.6 (CH_3), 67.2 (s, $C_4H_8O_2$), 145.8 s (*C*=CH_2) ppm. The (probably very broad) signal for CH_2 is missing due to low concentration.

NMR spectra of $[InCl_2(C_3H_5)]$ (3a)

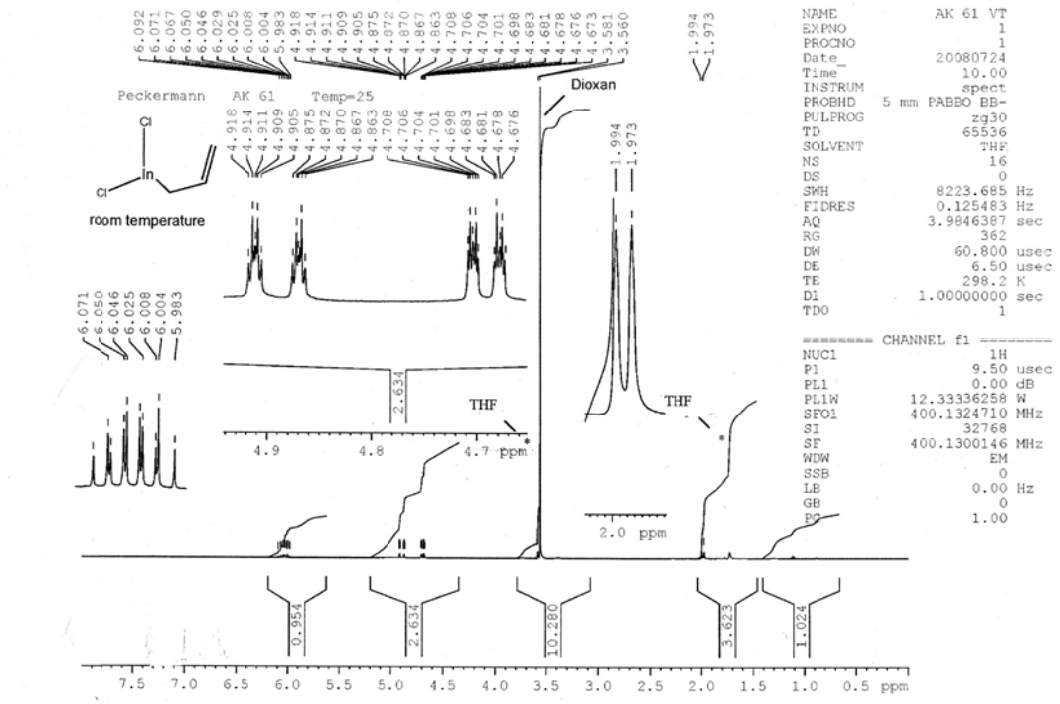

Figure S21: ^{1}H-NMR spectrum of **3a** (THF-d^8, –75°C)
δ = 2.00 (d, 2 H, J = 8 Hz, $InCH_2$), 3.54 (**s**, $C_4H_8O_2$) 4.68 (dd, 1 H, J_{cis} 10 Hz, J_{gem} 2 Hz, CH=C*H*H), 4.90 (ddt, 1 H, J_{trans} = 17 Hz, J_{gem} = 2 Hz, ^{3}J = 1 Hz, CH=CH*H*), 6.01 (m, 1 H, CH) ppm.

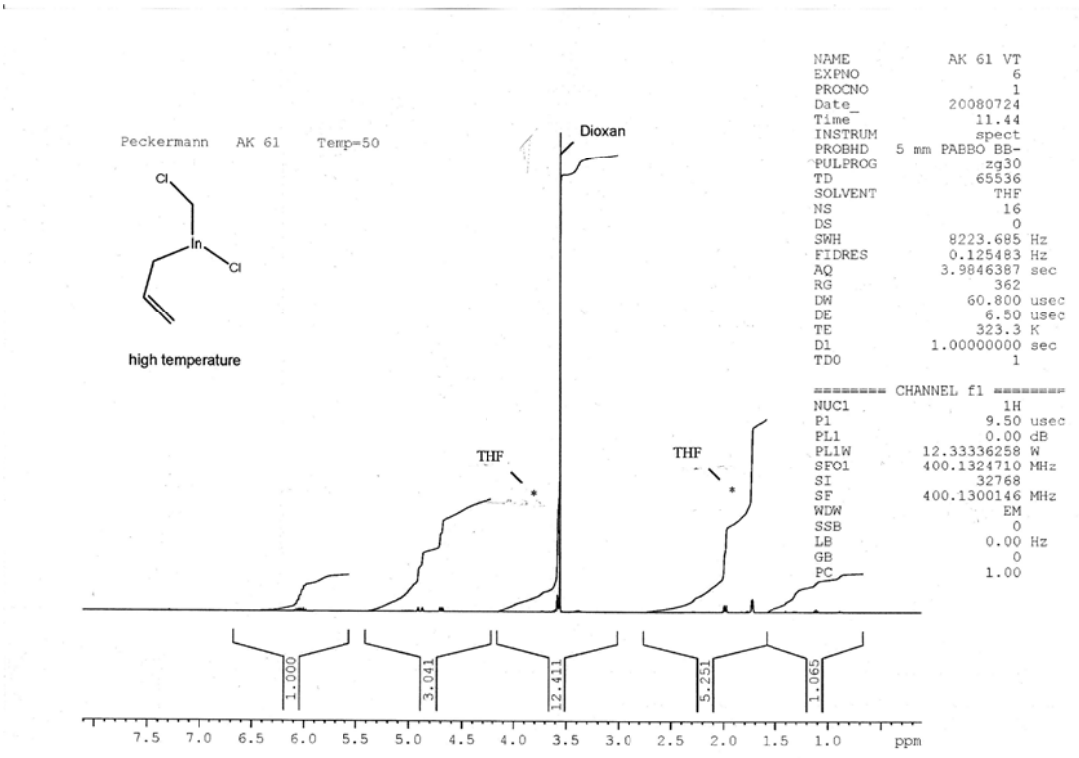

Figure S22: ^{1}H-NMR spectrum of **3a** (THF-d^8, +25°C)
δ = 2.00 (d, 2 H, J = 8 Hz, $InCH_2$), 3.56 (**s**, $C_4H_8O_2$) 4.70 (ddm, 1 H, J_{cis} 8.4 Hz, J_{gem} 2 Hz, CH=C$_H$H), 4.90 (ddm, 1 H, J_{trans} = 12 Hz, J_{gem} = 1.2 Hz, CH=CH*H*), 6.04 (m, 1 H, CH) ppm.

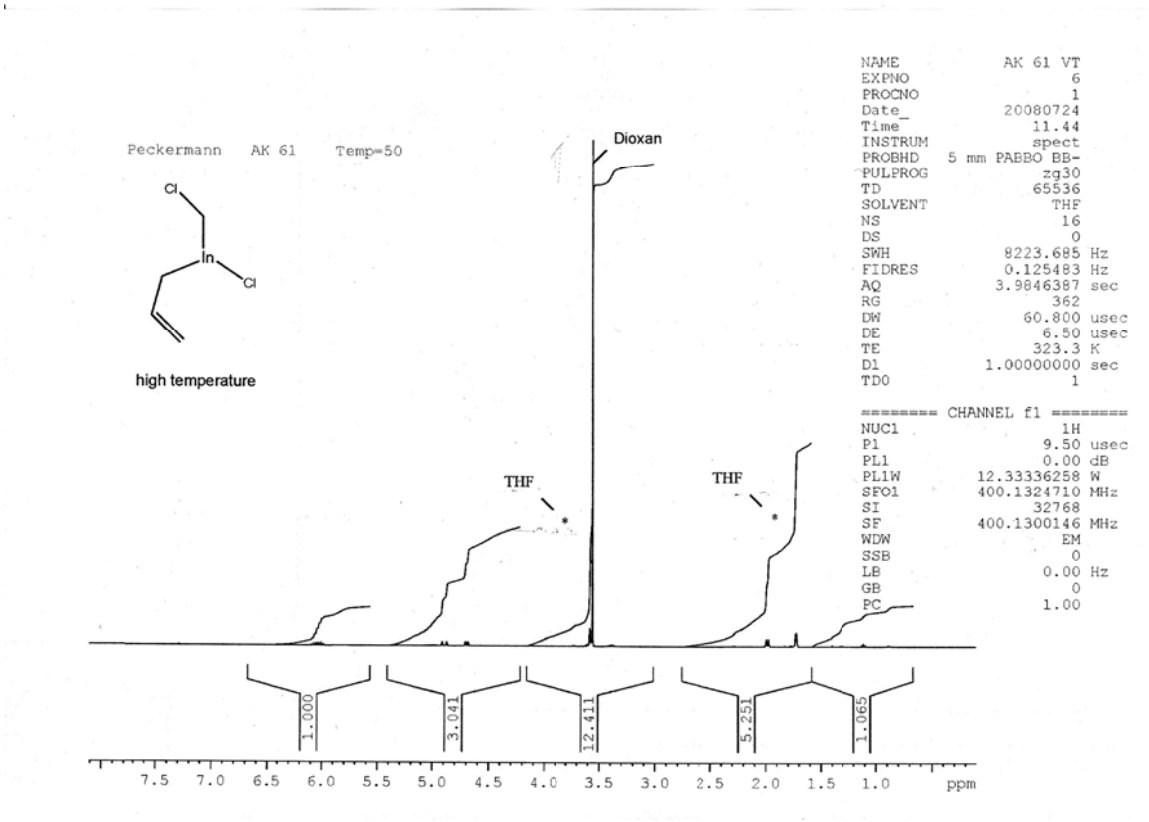

Figure S23: ^{1}H-NMR spectrum of **3a** (THF-d^{8}, +50°C)
No changes are observed compared to the spectrum at room temperature (see above).

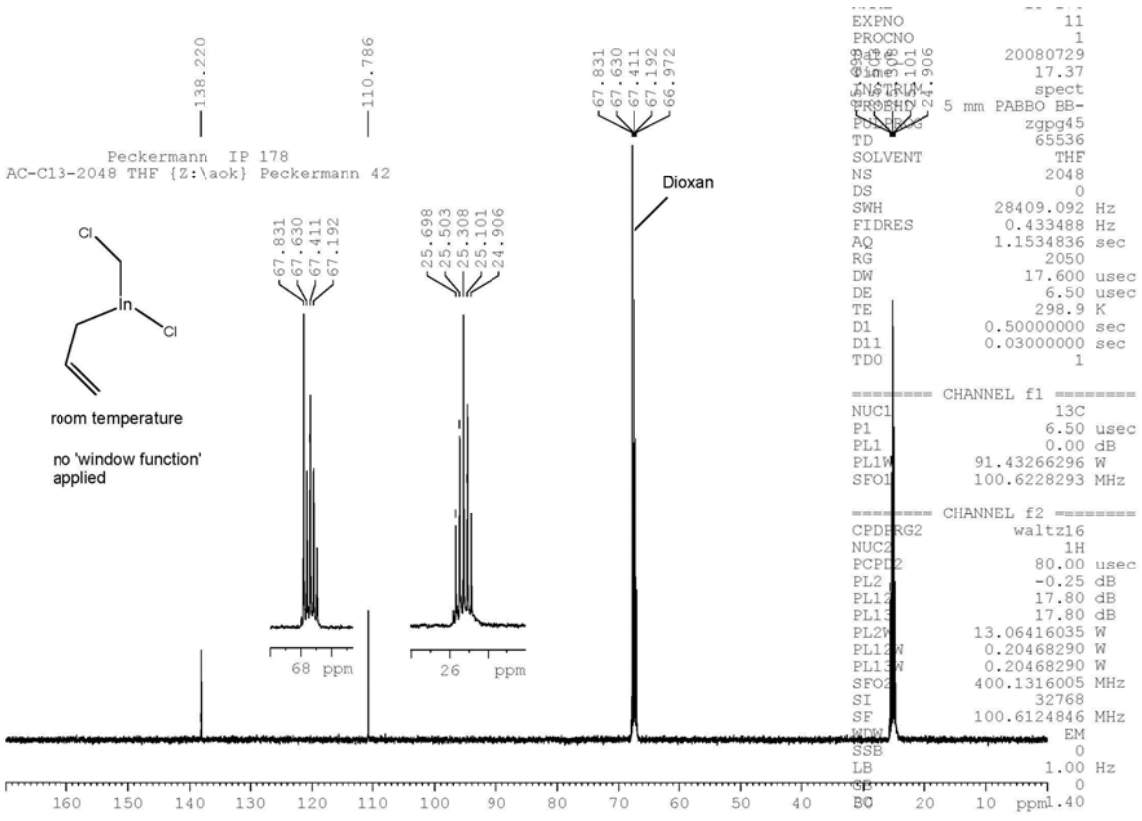

Figure S24: ^{13}C{^{1}H}-NMR spectrum of **3a** (THF-d^{8}, +26°C)
δ = 25.3 (br, $InCH_2$), 67.8 ($C_4H_8O_2$), 110.8 (s, $CH{=}CH_2$), 138.2 (s, CH) ppm.

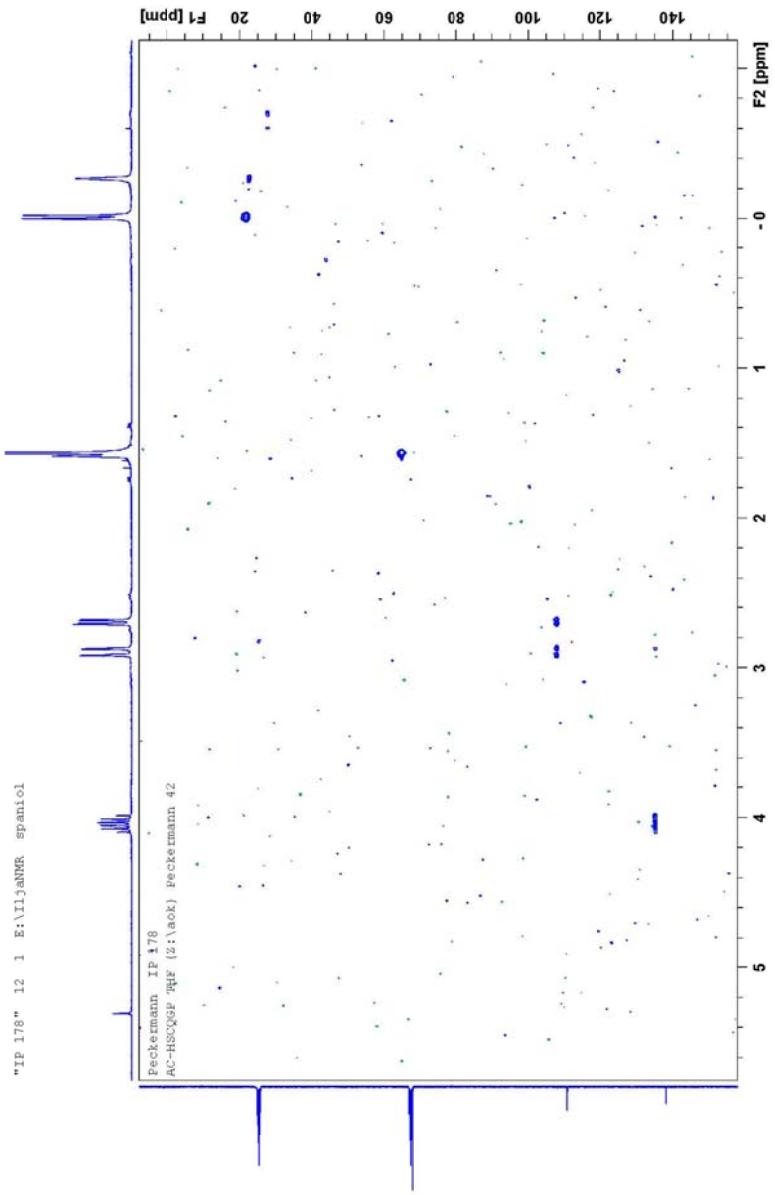

Figure S25: HSQC-NMR spectrum of **3a** (THF-d^8, +27°C)
(proving the assignment of the CH2 signal in the ^{13}C NMR spectrum at 25 ppm)

NMR spectra of [$InCl_2(C_4H_7)$] (3b)

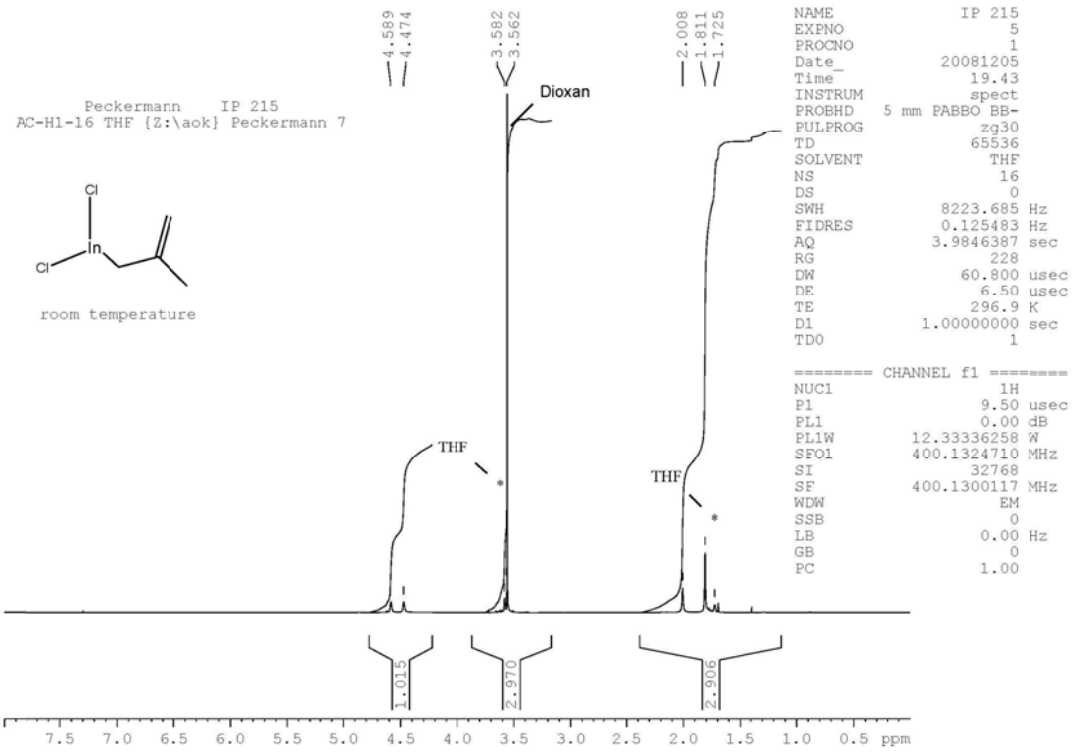

Figure S26: ^{1}H-NMR spectrum of **3a** (THF-d^8, +24°C)
δ = 1.81 (s, 3 H, CH_3), 2.01 (s, 2 H, $InCH_2$), 3.56 (s, $C_4H_8O_2$), 4.47 (s, 1 H, CH=C*H*H), 4.59 (s, 1 H, (s, 1 H, CH=CH*H*) ppm.

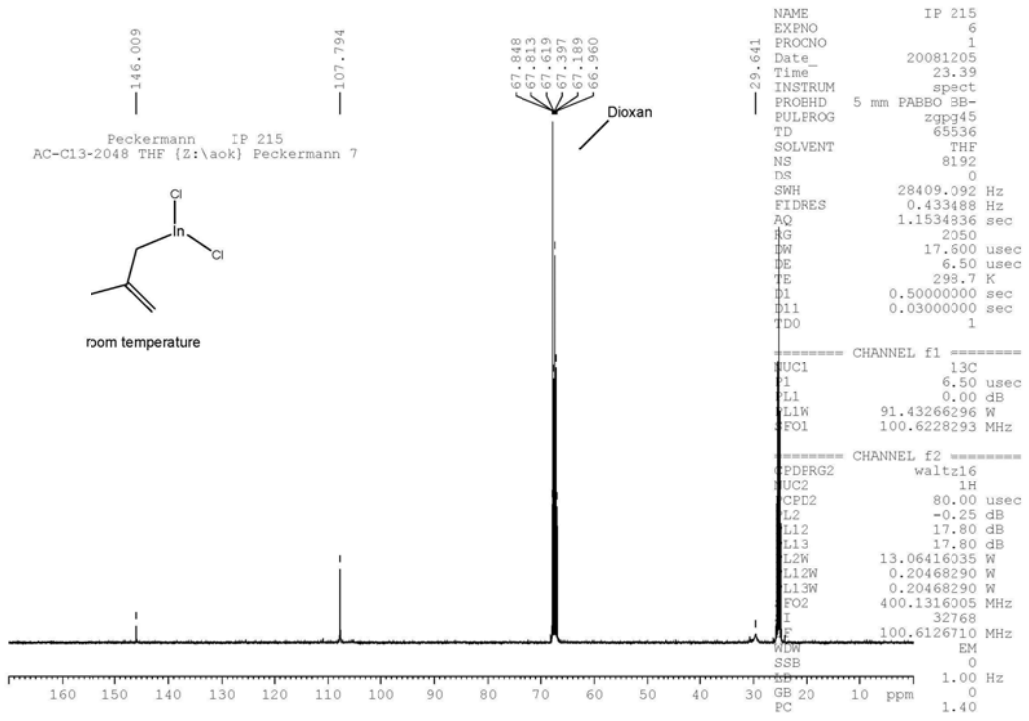

Figure S27: ^{13}C{^{1}H}-NMR spectrum of **3b** (THF-d^8, +26°C)
δ = 25.2 (br, $InCH_2$, covered by the signal of THF), 29.6 (br s, CH_3) 67.4 ($C_4H_8O_2$), 107.8 (s, CH=CH_2), 146.0 (s, CH) ppm.

Crystal structure determination of 1a, 1b and 4

Due to the air sensitivity of compounds **1a**, **1b** and **4**, the crystals of all three compounds were frozen in paratone oil. The crystals were taken from their Schlenk tubes using as spatula and were immediately sticked into the oil and transferred to the diffractometer (where the oil was frozen on top of a needle). All data collections were carried out using a Bruker diffractometer with Incoatec microsource and an Apex area detector with Mo-Kα radiation (λ = 0.1073 Å). Absorption corrections were performed with the program SADABS.[1] The structures were solved by direct methods (SIR-97),[2] completed by subsequent Fourier syntheses and refined with full-matrix least-squares methods against $|F^2|$ data using SHELXL as incorporated in the program system WinGX.[3,4] All non-hydrogen atoms were refined anisotropically, except for the carbon atoms C10, C11 and C12 in compound **4** that were refined with split positions and isotropic displacement parameters. The hydrogen atoms of the allyl ligands in **1a** were refined in their position; the hydrogen atoms that belong to the dioxane ligand were included in calculated positions and treated as riding. The hydrogen atoms in **1b** were refined in their position except of those attached to C8 and C12 (methyl groups) that were included in calculated positions. All hydrogen atoms in **4** were included in calculated positions and treated as riding. All crystallographic figures were prepared using DIAMOND.[5]

1 Siemens. ASTRO, SAINT and SADABS. Data Collection and Processing Software for the SMART System. Siemens Analytical X-ray instruments Inc., Madison, Wisconsin, USA, 1996.
2 A. Altomare, M. C. Burla, M. Camalli, G. L. Cascarano, C. Giacovazzo, A. Guagliardi, A. G. G. Moliterni, G. Polidori, R. spagna, *J. Appl. Cryst.* 1999, **32**, 115.
3 L. J. Farrugia, WinGX, *J. Appl. Cryst.* 1999, **32**, 837.
4 G. M. Sheldrick, *Acta Crystallogr. A*, 2008, **64**, 112.
5 K. Brandenburg, H. Putz, *Diamond - Crystal and Molecular Structure Visualization*, Crystal Impact, Rathausgasse 30, D-53111 Bonn, Germany.

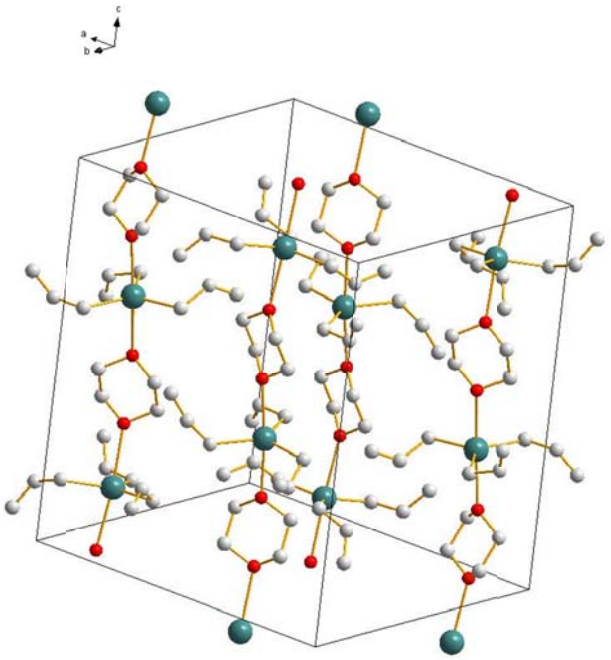

Figure S28: DIAMOND representation of **1a** showing the crystallographic packing. Displacement ellipsoids set at 50%; hydrogen atoms omitted for clarity.

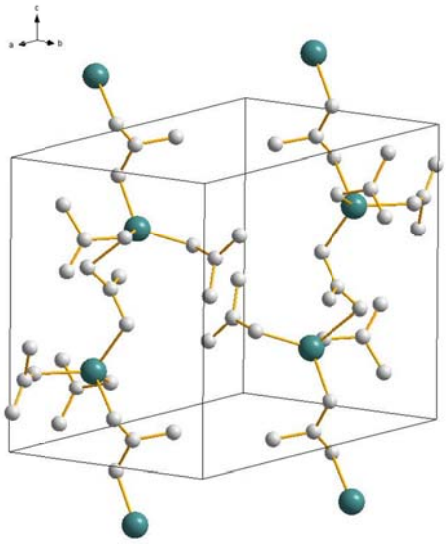

Figure S29: DIAMOND representation of **1b** showing the crystallographic packing. Displacement ellipsoids set at 50%; hydrogen atoms omitted for clarity.

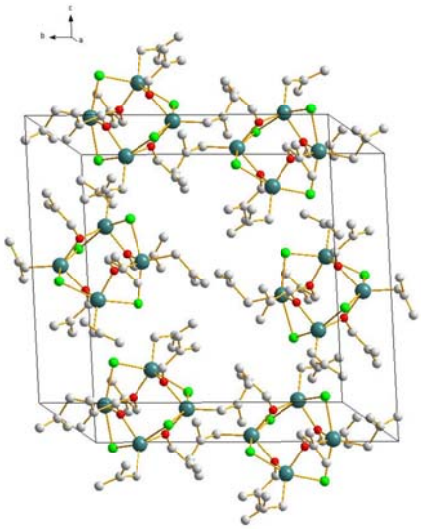

Figure S30: DIAMOND representation of **4** showing the crystallographic packing. Displacement ellipsoids set at 50%; hydrogen atoms omitted for clarity.

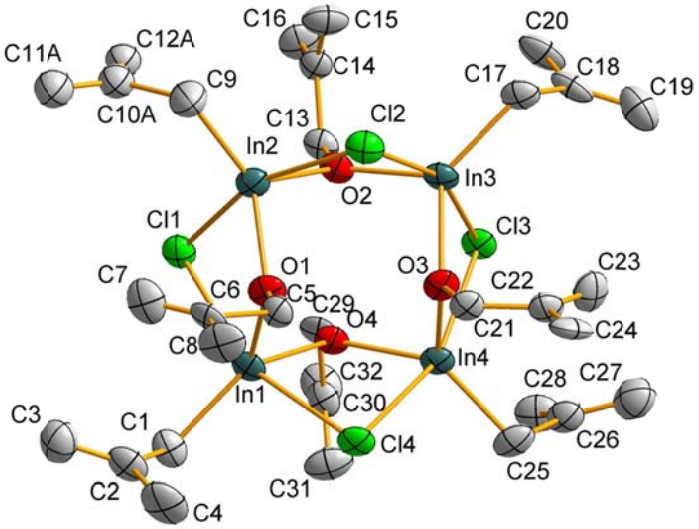

Figure S31: ORTEP diagram of the molecular structure of **4**. Displacement ellipsoids set at 50%; hydrogen atoms omitted for clarity. Only one of the split positions for the atoms C10A, C10B, C11A, C11B, C12A, and C12B are shown. Selected interatomic distances [Å] and angles [°]: In1...In2 3.5313(15), In2...In3 3.5404(15), In3...In4 3.5354(14), In1...In4 3.5476(15), In1...In3 5.0052(18), In2...In4 5.004(2), In1...In2...In3 90.11(4), In2...In3...In4 90.01(4), In1...In4...In3 89.93(4), In2...In1...In4 89.96(4), C1–C2 1.457(15), C2–C3 1.357(19), C2–C4 1.450(17), C5–C6 1.502(16), C6–C7 1.283(18), C6–C8 1.504(16), C9–C10A 1.61(3), C9–C10B 1.46(4), C10A–C11A 1.29(4) , C10A–C12A 1.50(3), C10B–C11B 1.30(5) , C10B–C12B 1.44(5), C13–C14 , C14–C15 1.321(18), C14–C16 1.482(15), C17–C18 1.508(16), C18–C19 1.30(2), C18–C20 1.474(18), C21–C22 1.468(17), C22–C23 1.306(17), C22–C24 1.497(16), C25–C26 1.456(16), C26–C27 1.35(2), C26–C28 1.481(17), C29–C30 1.500(17), C30–C31 1.314(17), C30–C32 1.488(15), C1–C2–C3 123.2(12), C1–C2–C4 117.4(13), C3–C2–C4 119.4(13), C4–C6–C7 123.5(11), C5–C6–C8 111.4(11), C7–C6–C8 125.2(12), C9–C10A–C11A 119(2), C9–C10A–C12A 119.7(19), C11A–C10A–C12A 121(3), C9–C10B–C11B 128(4), C9–C10B–C12B 105(3), C11B–C10B–C12B 127(4), C13–C14–C15 121.1(11), C13–C14–C16 113.6(11), C15–C14–C16 125.2(12), C17–C18–C19 121.2(13), C17–C18–C20 115.2(13), C19–C18–C20 123.6(13), C21–C22–C23 124.9(11), C21–C22–C24 111.9(11), C23–C22–C24 123.2(13), C25–C26–C27 123.2(13), C25–C26–C28 115.9(13), C27–C26–C28 120.9(13), C29–C30–C31 123.9(11), C29–C30–C32 112.2(10), C31–C30–C32 123.9(13).